Experimental and Numerical Comparison of Lead-Free and Lead-Containing Brasses for Fixture Application

G. Radzioch [a, b, *], D. Bartocha [a] ⓘD, M. Kondracki [a] ⓘD

[a] Department of Foundry Engineering, Silesian University of Technology, 7 Towarowa Str. 44-100 Gliwice, Poland
[b] Joint Doctoral School, Silesian University of Technology, 2A Akademicka Str. 44-100 Gliwice, Poland
* Corresponding author: E-mail address: grzegorz.radzioch@polsl.pl

Abstract

A comparative analysis of brasses alloys, namely lead-free CuZn (CB771) and lead containing CuZn (CB770), was conducted in this article. The results of the comparative analysis and experimental investigations aimed to provide comprehensive knowledge about the thermophysical properties and solidification characteristics of these alloys. Thermodynamic simulations using Thermo-Calc software and modifications in the chemical composition of the CB771 alloy were employed to approximate its characteristics to those of the lead containing CuZn alloy. Thermal-derivative analysis of the alloys and a technological trial were carried out to determine their solidification characteristics, fluidity, and reproducibility. The casting trials were conducted under identical conditions, and the results were compared for a comprehensive analysis. Additionally, a solidification process simulation was performed using MagmaSoft software to match the thermophysical properties. The aim of this research was to achieve maximum consistency between the simulation results and experimental investigations.

Keywords: Lead-Free Brass, ATD, Shrinkage, Simulation, Validation

1. Introduction

For the production of pipes, valves, and sanitary fittings, due to their excellent corrosion resistance, copper alloys with zinc, commonly called brass, are used. The CuZn alloy with a lead content of up to 1.6% has found the widest application due to its good technological properties, such as good castability and machinability. However, the toxic nature of lead is increasingly being recognized and emphasized by authorities worldwide, leading to a trend of reducing this element in products in contact with drinking water. [1,2]

Reducing the lead content to below 0.1% results in a significant decrease in casting properties (castability, reproducibility) and susceptibility to mechanical processing (machinability). At the same time, there is an increased tendency to form shrinkage and surface defects [3-5]. The members of the Joint Committee of Four Member States (4MS) of the European Association of Valve and Fitting Manufacturers are introducing further restrictions on the allowable amounts of Pb and Ni in brass alloys in contact with drinking water, promoting the development of new lead-free brass alloys. [6,7]

To achieve the long-term goal of phasing out leaded brass alloys from infrastructure, it is necessary to increase this basic knowledge. This article aims to contribute to this effort by examining how the chemical composition, especially decreasing the lead content, contributes to the casting properties of brass.

2. Methodology

The data from the chemical composition certificate of the CB771 brass provided by the manufacturer were utilized to conduct phase transformation simulations using Thermo-Calc software. These simulations aimed to determine the path of changes in the

chemical composition of the lead-free brass alloy, bringing it closer to the characteristics of the lead containing CuZn alloy (CB770). Based on the results of the phase transformation simulations in Thermo-Calc, modifications were made to the CB771 brass alloy by increasing the proportions of zinc and tin.

The research was carried out in the form of thermal-derivative analysis (TDA) on the CB770 and CB771 brass alloys, with experimental castings conducted in standard TDA cups (Figure 1). The research material was directly obtained from ingots and then melted in a crucible furnace, raising the brass temperature to 1010°C. Simultaneously, thermal-derivative analysis was performed on the newly developed alloy with higher tin and zinc content, maintaining the same casting conditions and parameters. The study aimed to determine the solidification and crystallization characteristics of the aforementioned CuZn alloys, along with their comparative analysis.
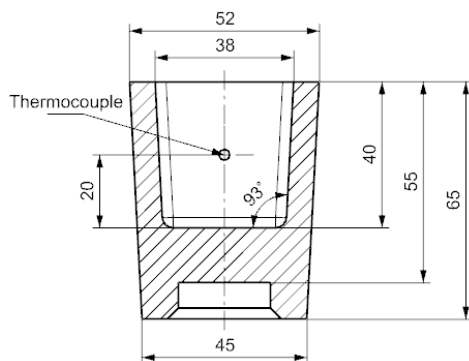

Fig. 1. Geometry of TDA tester

To assess the fluidity and reproducibility of the investigated brass alloys, a technological trial proposed by J. Navarro-Alcacero was employed. The dimensions of the test casting, excluding the gating system, are presented in Figure 2. Within the comb test, fluidity is measured by the relative length of metal filling in the horizontal main channel until its solidification. Reproducibility, on the other hand, is identified by the relative length of the main channel when the triangular side notches are completely filled with liquid metal [8].

All experimental castings were conducted in a permanent cast iron mould, maintaining identical casting conditions for all cases. To ensure result comparability, measurements were performed at the same pouring temperatures for all representative samples. The analysis of the conducted technological trial will allow for the determination of the flow characteristics of the alloy in the mould and a precise comparison of different samples in terms of their fluidity and reproducibility.
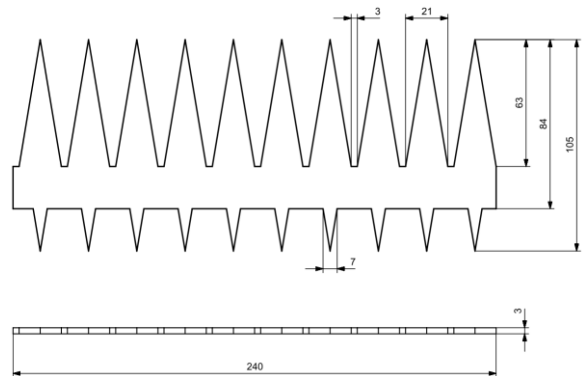

Fig. 2. Dimensions of the Navarro-Alcacero technological sample casting

To investigate the tendency of the alloys to form so-called shrinkage defects, a cone test was conducted. [9] For this purpose, a shell mould, commonly used in TDGA (Thermal Derivative Gravimetric Analysis) studies, was utilized, and its cross-section is presented in Figure 3. An analysis of castings with identical cone dimensions was carried out while maintaining consistent pouring parameters. The mould temperature was set at 23°C, the temperature of the liquid metal was 1030°C, and the pouring rate was kept constants for all representative samples. To assess susceptibility to shrinkage, two types of samples were prepared. One of them was covered with insulating material made of aluminosilicate immediately after pouring, while the other was left without insulation during the solidification process.
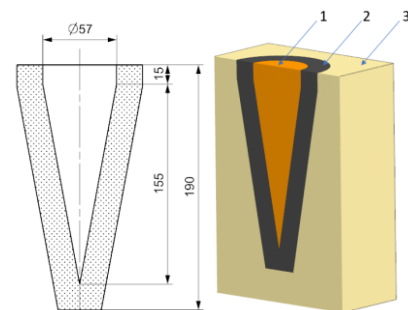

Fig. 3. Casting geometry of cone shape probe 1- cone cast, 2- shell mould, 3- sand

Based on the obtained cooling and crystallization curves, the thermophysical properties of the CB771 brass alloy were determined. MagmaSoft software was utilized to match these properties through validation. A simulation of the alloy solidification process in a standard ATD cup was conducted to closely replicate the real process. The cooling curve from the simulation was compared with the results of experimental investigations, and appropriate modifications were made to the numerical model of the alloy. The aim of these modifications was to achieve maximum consistency between the cooling and crystallization curves obtained from the simulation and thermal-derivative analysis. Another objective was to attain comparable results in terms of porosity.

3. Development of new alloy composition

The analysis of the chemical composition of lead-free brass, designated as CB771S in the delivery state, shows that it is excessively free of impurities of elements that have an influence on the structure and casting properties of the alloy (Table 1). Additionally, the level of zinc is kept relatively low. The chemical composition in this form promotes:
– an increase in the liquidus temperature,
– an extension of the range of solidification temperatures,
– the possibility of discontinuities in the structure due to increased shrinkage and hot cracking,
– the possibility of unstable primary crystallization involving the α phase, and a reduction in hardness below the minimum required by the standard.

Table 1.
Alloy composition in delivery state. Data from producer certificate

CB771	Cu	Zn	Pb	Sn	Fe	Al
	63.4%	35.9%	0,1%	0,02%	0,07%	0,52%
	Ni	Mn	Si	Sb	As	B
	0,002%	0,001%	0,003%	0,04%	0,03%	6ppm

The statement has been confirmed by phase transformation analyses conducted using Thermo-Calc software. The following images (Figures 4, 5) indicate that with an increase in the zinc content the liquidus temperature of the alloy increases, while the range of solidification temperatures gradually decreases. A similar phenomenon was also observed in the case of changing the aluminium content. Table 2 presents the chemical compositions of the investigated alloys, including the newly developed CuZn alloy with a higher content of tin and zinc. The effective copper content was calculated using the de Guillett formula (1).

$$Cueff = \frac{100*Cu}{100-Pb+(9*Si)+(5*Al)+Sn-(0,1*Fe)-(0,5*Mn)-(1,3*Ni)} \quad (1)$$
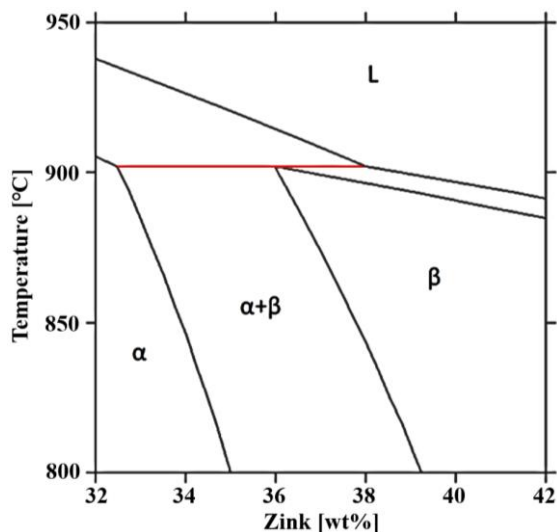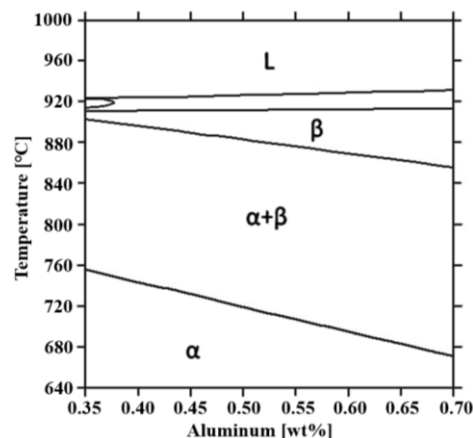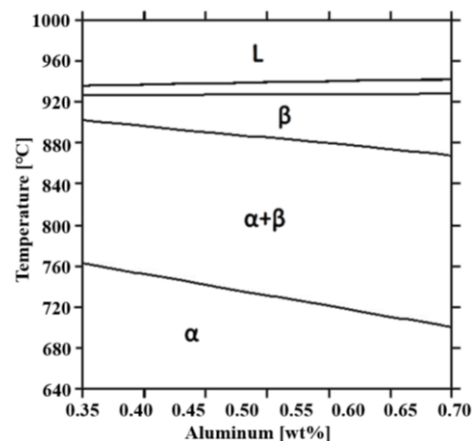

Fig. 4. TC calculated the phase transformation diagram for variable zinc content without additional alloying elements
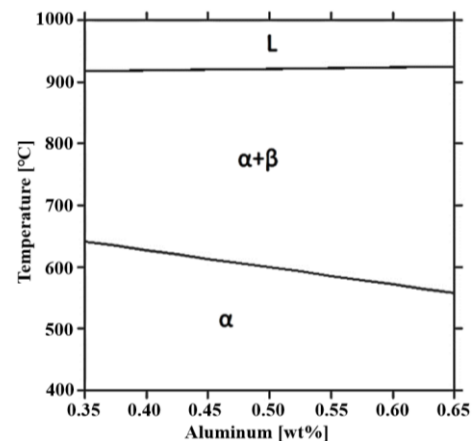
a)

b)

c)

Fig. 5. Phase transformation charts for varying aluminium content and different levels of zinc. a) Zn – 34%, b) Zn – 35% and c) Zn – 36%

Table 2.
Alloy composition measured on Bruker Q8 Magellan spectrometer

	Name/Element	Cu [%]	Zn [%]	Pb [%]	Sn [%]	Fe [%]	Al [%]	Ni [%]	Mn [%]	Si [%]	As [%]	Sb [%]	B [ppm]	Cueff [%]
P1	CB770	62.35	35.81	0.89	0.046	0.078	0.645	0.053	0.002	0.007	0.080	0.006	9	60.91
P2	CB771	64.3	34.9	0.088	0.021	0.076	0.500	0.002	0.001	0.003	0.030	0.039	10	62.80
P3	CB771↑Zn↑Sn	62.07	36.86	0.088	0.255	0.069	0.565	0.002	0.001	0.003	0.028	0.032	10	60.26

4. Thermal and Derivative Analysis

The thermal and derivative analysis (TDA) method was employed to analyse the solidification and crystallization processes. The study was conducted using a commercial METACUP C sample. The use of a sample with uniform wall thickness around the test castings ensures unidirectional, radial heat flow. The heat centre of the test castings coincides with their geometric centre, where a type K thermocouple was placed.

The thermal curve $T = f(t)$ and its derivative curve, referred to as the crystallization curve $T' = dT/dt = f'(t)$, recorded during the solidification of the metal in the test sample, were subjected to analysis according to the presented scheme in Figure 4. The analysis involved determining characteristic points on the curves and was performed for each alloy sample. The aim of the analysis was to identify the temperature values corresponding to specific phases of the casting solidification.

The alloys were divided into groups based on their lead content, where CB770S contained 1% of this element, CB771S contained 0.1% of lead, and the third alloy was a lead-free brass with modified chemical composition, with an increased content of zinc and tin by 0.25%. It is important to emphasize that the modified alloy still meets the required specifications.

The analysis of the solidification and crystallization curves of the investigated CuZn alloys, considering temperature values, derivative values, and characteristic point times, provided significant information regarding key parameters of the solidification process, enabling the identification and appropriate classification of points of particular significance. Starting from the beginning of solidification, point A indicates this stage. The next crucial point is B, indicating a change in solidification kinetics and concurrent stabilization of β phase precipitation. The maximum thermal effect associated with β phase precipitation, corresponding to the liquidus temperature, is represented by point C. The process of β phase crystallization occurs in the C-D region, within the temperature range of T_{liq} and T_{sol}. Point E represents the thermal effect associated with the solidus temperature. Subsequently, point F signifies the completion of the solidification process. In further analysis, point G indicates the beginning of β→α+β phase decomposition. Point H denotes the maximum thermal effect associated with β→α+β phase decomposition. Point I mark the completion of this decomposition. Another important point is J, signifying the beginning of β→β' phase ordering. Point K represents the maximum thermal effect associated with this ordering process. Finally, point L indicates the end of β→β' ordering. An example of the ATD curves with marked characteristic points, subjected to the described analysis, is shown in Figure 6. The ATD curves for CB771 brass and its modified version are presented in Figure 7.
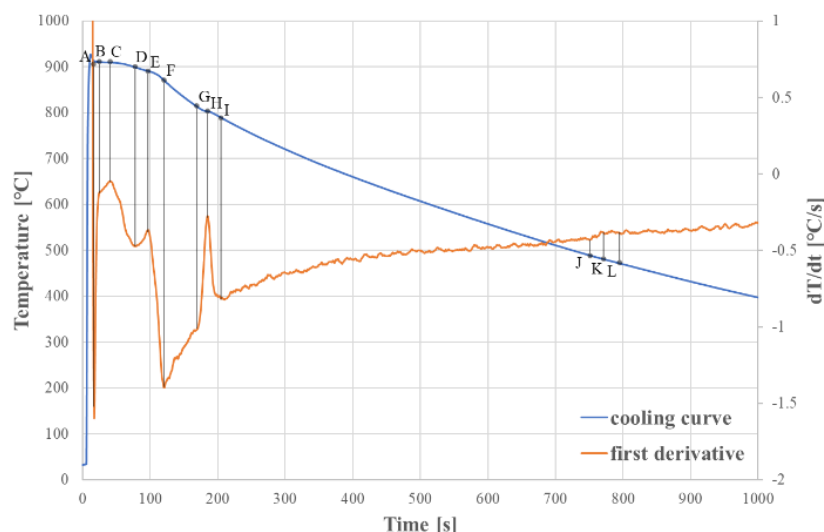

Fig. 6. Method of characteristic temperatures determination on the base of solidification and crystallization curves for CB770 alloy
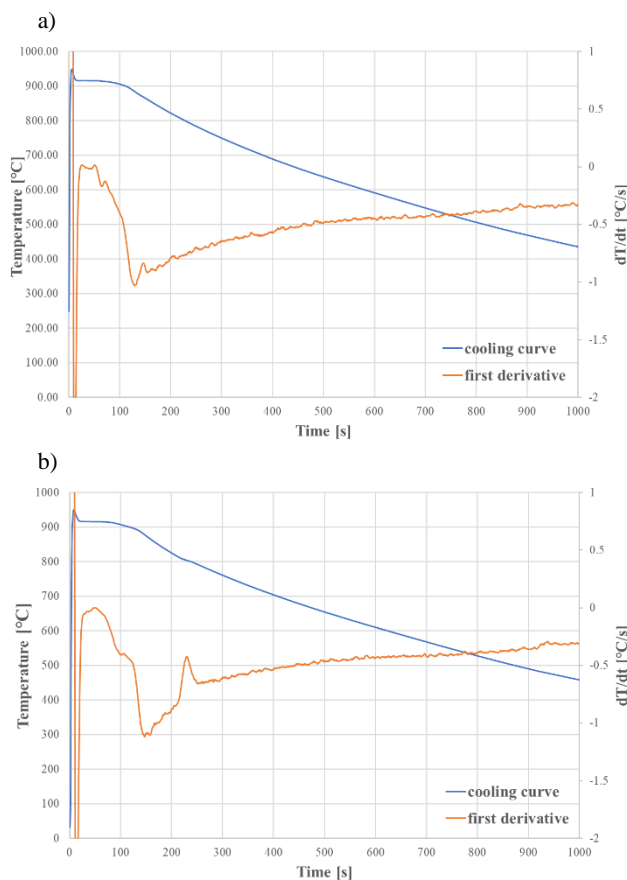
a)

b)

Fig. 7. Solidification and crystallization curves. a) CB771S in delivery state, b) modified brass CB771

Based on the provided data (Table 3), several conclusions can be drawn regarding the investigated alloys:

All tested alloys exhibit relatively high liquidus temperatures. Alloy P1 shows the lowest liquidus temperature, which is 909.7°C. Lead-free brasses P2 and P3 have higher liquidus temperatures, specifically 915.8°C and 915.2°C, respectively.

The solidus temperature also differs depending on the tested alloys. Alloy P1 exhibits the lowest solidus temperature, which is 892.3°C, while P2 and P3 are characterized by higher solidus temperatures, specifically 912.9°C and 904.5°C, respectively.

In terms of the temperature of the β→α+β decomposition onset, it is observed that P1 has the lowest onset temperature, which is 809.4°C, while P2 exhibits a higher temperature of 873.5°C. The addition of Zn and Sn to alloy P2 results in a decrease in the β→α+β decomposition onset temperature to 821.4°C.

Regarding the temperature of the β→β' ordering onset, which indicates the moment when ordering of the alloy structure into α and β' phases occurs, it was found that P1 has a higher α+β' ordering onset temperature of 486.8°C compared to P2, which has a temperature of 478.1°C. The addition of Zn and Sn to P2 slightly increases the α+β' ordering onset temperature to 483°C.

Special attention should be paid to the time between the liquidus temperature (point C) and the solidus temperature (point E), which is a significant factor to consider. A more than two-fold reduction in solidification time was observed for lead-free brass P2 compared to P1. Additionally, increasing the percentage of zinc and tin in the lead-free brass allowed for a closer approximation of the solidification time to the level observed in the case of P1.

The obtained results confirm the earlier calculations carried out using the Thermo-Calc program.

Table 3.
Coordinates of the characteristic points on the ATD charts

	P1 - CB770			P2 - CB771			P3 - CB771 ↑Zn ↑Sn		
Point	Time	Temperature	dT/dt	Time	Temperature	dT/dt	Time	Temperature	dT/dt
A	17	913.3	-1.598	9	935.5	-1.158	11	941.4	-1.299
B	30	910.4	-0.100	22	915.8	-0.017	32	915.6	-0.043
C	38	909.7	0.055	56	915.8	-0.038	47	915.2	0.000
D	83	897	-0.465	61	915.4	-0.138	98	907.7	-0.398
E	94	892.3	-0.387	77	912.9	-0.179	106	904.5	-0.399
F	118	874.8	-1.349	128	886.4	-0.986	151	873.4	-1.093
G	174	809.4	-0.920	141	873.5	-0.893	204	821.4	-0.857
H	182	803.9	-0.364	144	871	-0.852	232	802.7	-0.435
I	202	792.2	-0.799	160	856.7	-0.895	257	788	-0.651
J	757	486.8	-0.414	874	478.1	-0.364	920	483	-0.338
K	777	479	-0.390	883	474.9	-0.338	940	476.8	-0.303
L	801	469.8	-0.387	902	468.5	-0.340	945	475.2	-0.315

5. Castability and susceptibility to shrinkage

The flowability and mould filling property are crucial in the process of casting alloys. In the case of brass alloys, the addition of lead aims to improve these properties. To assess the impact of the absence of lead on the fluidity of the alloy, a fluidity analysis was conducted based on the results of a comb test.

Measurements were carried out for the brass alloys CB770S, CB771S, and lead-free brass with increased zinc and tin content at different casting temperatures: 1030°C, 1020°C, 1000°C. Test castings with specified dimensions were made in the same permanent cast iron mould for all investigated cases. The measurement results are presented in Table 4.

The analysis of fluidity and mould fillability revealed a clear negative impact of reduced pouring temperature on the fluidity of CuZn alloys. Interestingly, in the case of lead-free brass alloys, an apparent improvement in fluidity was observed compared to the CB770S brass, which contains 0.9% lead.
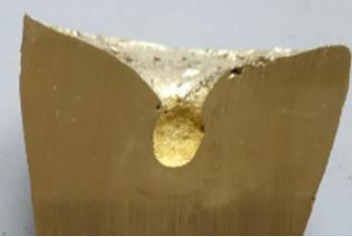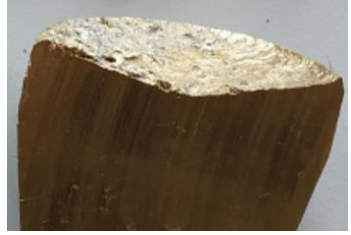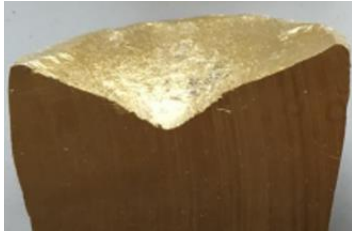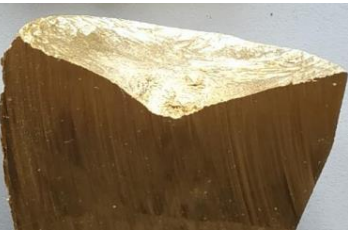
This phenomenon is attributed to the localized precipitation of the α phase during solidification, resulting in partial remelting of the already solidified metal due to the heat released during the phase transformation. These conditions promote better flow of the liquid metal in the mould, but unfortunately, they do not lead to complete filling of the mould cavity, resulting in a significant decrease in mould fillability.

The conclusion drawn from the analysis highlights the significance of lead presence in brass alloys in terms of fluidity and mould fillability. The absence of lead has a negative impact on these properties of the alloy, which can have significant consequences in the casting process, especially at lower pouring temperatures.

Table 4.
The results of the combing test for castability

Casting Temperature	CB770S	CB771S	CB771 ↑Zn ↑Sn
1030°C			
1020°C			
1000°C			

Porosity is one of the main defects present in castings of all metal alloys. It poses a significant threat to the mechanical and functional properties of these castings. Porosity is caused by two simultaneous mechanisms: solidification shrinkage and gas segregation, albeit with varying intensities. The chemical composition of the alloy has a significant influence on the value of casting shrinkage, which is a key indicator in the casting formation process. Optimizing the chemical composition of the alloy and properly managing the solidification process are crucial factors in reducing porosity and improving the properties of castings, both in terms of mechanical and functional aspects. [10]

Axial cross-sectioning of cone-shaped samples was performed to analyse shrinkage and the formation of defects. During these tests, an interesting phenomenon was observed in the CB771S alloy, which showed a tendency to form a concentrated shrinkage cavity in the uncovered cone casting. To reduce this phenomenon, insulation was applied, which effectively contributed to the reduction of shrinkage cavity formation. However, a significant tendency to form such defects can still be observed compared to the CB770S alloy, which settles uniformly regardless of the use or absence of insulation in the upper part of the casting. Observation of the solidification in the cone casting of the CB771 alloy with increased zinc and tin content showed an intermediate state between CB770 and the original CB771 version. The shrinkage cavity forms centrally but is smaller than in the case of the CB771 alloy. The results of the cone test are presented in Table 5.

Table 5.
Result of cone shape probe

	CB770S	CB771S	CB771S ↑Zn ↑Sn
Without insolation			
With insolation			

6. Thermophysical properties - Validation

The main goal of modelling casting processes is to predict the quality of virtual castings by identifying potential porosity and describing the flow behaviour of the molten metal [11]. To perform reliable simulations of the casting and solidification process, appropriate input data is required. This data includes the three-dimensional geometry of the casting along with the gating system, pouring time, initial metal temperature, mould temperature, mould material, heat transfer coefficients between the casting and mould or casting and core, and thermophysical properties of the alloy obtained from a database [12]. However, due to the limited availability of commercial databases for copper alloys, this study focused extensively on the thermophysical properties of the investigated alloy. By analysing the solidification and crystallization curves obtained from experimental studies, significant points where phase transformations occur can be detected (Figure 6). This enables the estimation of thermophysical properties to ensure more accurate simulations [13,14].

Both experimental and simulation studies were conducted on cast samples made of lead-free brass CB771S, whose chemical composition is presented in Table 2. The experiments were performed using standard TDA cups (Figure 8). A 3D model of the experimental measurement setup, including the sample and TDA cup, was designed in a CAD environment, and the 3D geometry was converted to the stl format and imported into the MagmaSoft 5.5.1 simulation system.

Boundary condition parameters were determined, including ambient temperature, radiation, and data related to the sand mould. Furthermore, the analysed thermophysical properties of the alloy were modified based on the results of the thermal analysis. All of these parameters were configured as input data for conducting the simulation study.

Fig. 8. The views of the test CB771S. CAD geometry of DTA cup using for simulations (left) and result of PT method after cutting (right)

The aim of the simulation study was to adjust the thermophysical data of the CB771 alloy in such a way that the cooling curve and its first derivative (crystallization curve) obtained from the numerical analysis as closely as possible matched those curves derived from the thermal-differential analysis. The boundary conditions of the standard ATD cup were considered reliable, with the material "Shell Sand" selected from the MagmaSoft database. The HTC (Heat Transfer Coefficient) was assumed to be constant at 800 W/m^2*K.

Simulations were conducted on the above-mentioned cup using all available brass alloys in the MagmaSoft database. The closest matching cooling and crystallization curves, calculated from the numerical analysis, were achieved for the CuZn40 material. The overlaid curves for the numerical and experimental analyses are presented in Figure 9.
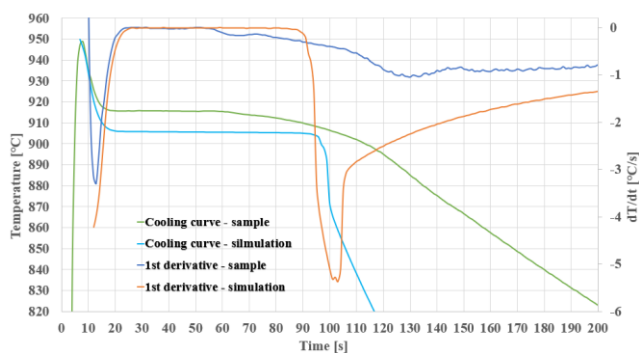
Fig. 9. Cooling and crystallisation curves from experiment and simulation CuZn40 alloy

Fig. 11. Cooling and crystallisation curves from experiment and simulation CB771 alloy after validation

Differences in the liquidus and solidus temperatures were observed. Additionally, the cooling dynamics of the alloy after reaching the solidus temperature were significantly higher compared to the experimental data. However, the cooling curve obtained from the numerical calculation matched the experimental characteristics, so based on this material from the database, a validation process was conducted. The thermophysical properties that underwent changes are:

- Liquidus temperature
- Solidus temperature
- Fraction solid (fs) as a function of temperature
- Density as a function of temperature
- Latent heat
- Heat conductivity as a function of temperature

For the newly developed material, a liquidus temperature of 915°C was assumed. The liquidus and solidus temperatures were read from the curve of the experimental thermal-differential analysis. The assumed liquidus temperature corresponds to point C (Table 3). The solidus temperature was taken as the end temperature of solidification registered in the experiment at point F (Table 3), which amounted to 886°C. A constant latent heat value was estimated at 200 kJ/kg. By changing these parameters and appropriately adjusting the fs and density curves as functions of temperature, a satisfactory match was achieved for the cooling and crystallization curves (Figure 11) as well as the porosity results (Figure 10), which are crucial for predicting potential casting defects.
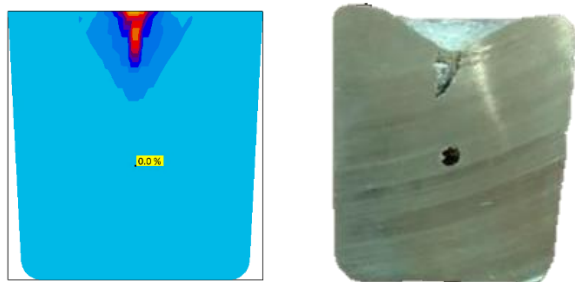
7. Conclusions

In summary, the conducted research on lead-free brass CB771 with lead content below 0.1% revealed significant differences in the solidification process compared to brass alloys containing around 1% lead. The thermal-differential analysis clearly confirmed much faster solidification of lead-free brass compared to its lead-containing counterpart.

To mitigate these differences, actions were taken to modify the composition of lead-free alloy CB771 by increasing the content of other alloying elements such as zinc and tin. This increase in the concentration of these alloying elements resulted in achieving a similar solidification process as in lead-containing brass.

However, it is important to note that the absence of lead in CuZn brass significantly lowers its casting properties. Regardless of the liquid metal temperature, a decrease in process reproducibility and increased susceptibility to shrinkage defects can be observed.

The thermal-differential analysis provides a sufficient amount of data that can be utilized for validation in simulation programs. This allows for the development of a material that closely approximates the actual thermophysical properties of lead-free brass CB771, enabling precise and reliable numerical calculations. Such research is of great importance for process optimization and the design of efficient systems that utilize lead-free brass CB771. Further research and development of this material can lead to its even more precise adaptation to specific applications, ensuring optimal thermophysical properties.

Acknowledgement

References

[1] Zoghipour, N., Tascioglu, E., Celik, F. & Kaynak, Y. (2022) - The influence of edge radius and lead content on machining

Fig. 10. Prognosis of shrinkage by MagmaSoft after validation(Left), Shrinkage from experiment (Right)

performance of brass alloys. Procedia CIRP. 112, 274-279. https://doi.org/10.1016/j.procir.2022.09.084.

[2] Hansen, A. (2019). Bleifreier rotguss als armaturen-undinstallationswerkstoff in der trinkwasserinstallation. *METALL Forschung*. 73(11), 452-455.

[3] Stavroulakis, P., Toulfatzis, A., Pantazopoulos, G. & Paipetis, A. (2022). Machinable leaded and eco-friendly brass alloys for high performance manufacturing processes: a critical review. *Metals.* 12(2), 246, 1-31. https://doi.org/10.3390/met12020246.

[4] Schultheiss, F., Johansson, D., Bushlya, V., Zhou, J., Nilsson, K. & Ståhl, J-E. (2017). Comparative study on the machinability of lead-free brass. *Journal of Cleaner Production.* 149, 366-377. https://doi.org/10.1016/j.jclepro.2017.02.098.

[5] Johansson, J., Alm, P., M'Saoubi, R., Malmberg, P., Ståhl, J-E. & Bushlya, V. (2022). On the function of lead (Pb) in machining brass alloys. *Journal of Advanced Manufacturing Technology.* 120, 7263-7275. https://doi.org/10.1007/s00170-022-09205-0.

[6] *Acceptance of metallic materials used for products in contact with drinking water, 4MS Common Approach Part B "4MS Common Composition List"* Retrieved July, 12, 2022 from http://www.umweltbundesamt.de/en/topics/water/drinking-water/distributing-drinking-water/guidelines-evaluation-criteria.

[7] Directive (EU) 2020/2184 of the European Parliament and of the Council of 16 December 2020 on the quality of water intended for human consumption, Dz.U.L 435/1 of 23.12.2020.

[8] Podrzucki, C. (1991). *Cast iron*. STOP. (in Polish).

[9] Cholewa, M., Suchoń, J., Kondracki, M. & Jura, Z. (2009). Method of thermal derivative gradient analysis (TDGA). *Archives of Foundry Engineering*. 9(4), 241-245. ISSN (1897-3310).

[10] Bruna, M. & Sladek, A. (2011). Hydrogen analysis and effect of filtration on final quality of castings from aluminium alloy AlSi7Mg0,3. *Archives of Foundry Engineering*. 11(1), 5-10.

[11] Ignaszak, Z. (2007). Validation problems of virtual prototyping systems used in foundry for technology optimization of ductile iron castings. *Advances in Integrated Design and Manufacturing in Mechanical Engineering II*, Springer, 57-79. https://doi.org/10.1007/978-1-4020-6761-7_4.

[12] Fajkiel, A., Dudek, P., Walczak, W. & Zawadzki, P. (2007). Improvement of quality of a gravity die casting made from aluminum bronze be application of numerical simulation. *Archives of Foundry Engineering*. 7(2), 11-14. ISSN (1897-3310).

[13] Persson, P-E., Ignaszak, Z., Fransson, H., Kropotkin, V., Andersson, R. & Kump, A. (2019). increasing precision and yield in casting production by simulation of the solidification process based on realistic material data evaluated from thermal analysis (Using the ATAS MetStar System). *Archives of Foundry Engineering*. 19(1), 117-126. DOI: 10.24425/afe.2019.127104.

[14] Ignaszak, Z. & Wojciechowski, J. (2020). Analysis and validation of database in computer aided design of jewellery casting. *Archives of Foundry Engineering*. 20(1), 9-16. DOI: 10.24425/afe.2020.131275.